

TOPS Nodal Code Solutions for the OECD/PBMR-400 Benchmark Problem

Jaejun Lee, Joo Hee Lee, Han Jong Yoo, Gil Soo Lee, and Nam Zin Cho
Korea Advanced Institute of Science and Technology
373-1 Kusong-dong, Yusong-gu, Daejeon, Korea; nzcho@kaist.ac.kr

Abstract

This paper provides the solution of the OECD/PBMR-400 benchmark problem by the TOPS code based on the Analytic Function Expansion Nodal (AFEN) method in 3-D cylindrical geometry. The paper is focused on the multi-group methodology, two methods (partial current translation and AFEN formulation) of treating the void regions, and comparison of the their results. We also suggest a modified benchmark problem, which does not have void regions where special treatments are required, to be used to verify the calculational methods in cylindrical geometry. The results indicate that the effect of void regions is significant and that the method how to treat the voids in computation is important.

KEYWORDS: *PBMR400, 3-D cylindrical geometry, AFEN, TOPS code, Void treatment, PCT*

1. Introduction

As an important candidate of very high temperature gas-cooled reactors (VHTRs), [1] the pebble bed type reactor is unique in its core configuration in that the core takes cylindrical shape and houses a multitude of graphite balls (containing many coated fuel particles) that are cycled continuously through the core several passes.

The Organization for Economic Cooperation and Development/Nuclear Energy Agency (OECD/NEA) issued a benchmark definition on the “OECD/NEA/NSC PBMR Coupled Neutronics/Thermal Hydraulics Transient Benchmark of the PBMR-400 Core Design,” [2] to advance state of the art in pebble bed reactor design analysis in general and to provide a forum for code-to-code comparisons of the benchmark results in particular.

This paper presents preliminary results of the TOPS nodal code solutions to this benchmark problem (steady state case exercise 1). The TOPS nodal code is based on the analytic function expansion nodal (AFEN) method recently developed in cylindrical (r, θ, z) geometry [3,4]. The AFEN methodology in this geometry as in hexagonal geometry is “robust”, due to the unique feature of the AFEN method that it does not use the transverse integration. The transverse integration in the usual nodal methods, however, leads to an impasse [5], that is, failure of the azimuthal term to be transverse-integrated over r - z surface.

The void regions in VHTR require proper treatments. Therefore, two special treatments such as partial current translation (PCT) and AFEN formulation are implemented in the TOPS code, and the results are presented in this paper.

The accurate solutions of the diffusion equation are not easy to come by in three-dimensional

cylindrical geometry containing void regions. A modified benchmark problem is suggested in Appendix to be used to verify various calculational methods and to ascertain the effect of the void regions.

2. Description of Method

Assume that the core in (r,θ,z) geometry is discretized into $N_r \times N_\theta \times N_z$ coarse nodes, where N_r , N_θ , and N_z are the numbers of divisions in radial, azimuthal, and axial directions, respectively. See Fig. 1. The AFEN formulation starts from the following multi-group diffusion equations in a homogenized node :

$$-\nabla^2 \vec{\phi}(r, \theta, z) + [\Lambda] \vec{\phi}(r, \theta, z) = 0, \tag{1}$$

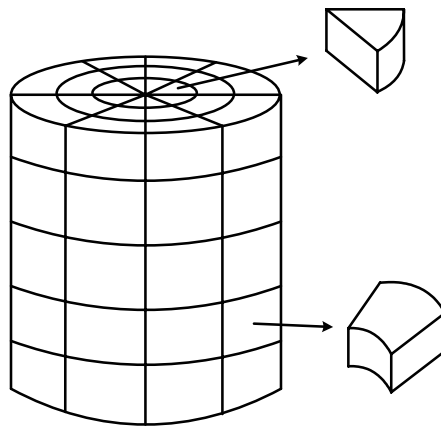
where

$$[\Lambda] = [D]^{-1} \left([\Sigma] - \frac{1}{k_{eff}} [\chi][\nu\Sigma_f] \right).$$

All the notations are standard. The equations can be written in the (r,θ,z) coordinate system as follows:

$$\frac{\partial^2 \vec{\phi}}{\partial r^2} + \frac{1}{r} \frac{\partial \vec{\phi}}{\partial r} + \frac{1}{r^2} \frac{\partial^2 \vec{\phi}}{\partial \theta^2} + \frac{\partial^2 \vec{\phi}}{\partial z^2} - [\Lambda] \vec{\phi} = 0. \tag{2}$$

Figure 1: Node shape in (r,θ,z) coordinate system



A general solution to Eq. (2) can be represented in terms of analytic basis functions that can be obtained using the method of separation of variables. For practical implementation, we choose the solution of a node expressed in a finite number of terms.

2.1 Outer Nodes

We use the following expression for an outer node:

$$\begin{aligned} \vec{\phi}(r, \theta, z) = & \vec{A}_0 + \sinh(\sqrt{[\Lambda]}z)\vec{A}_1 + \cosh(\sqrt{[\Lambda]}z)\vec{A}_2 \\ & + I_0(\sqrt{[\Lambda]}r)\vec{A}_3 + K_0(\sqrt{[\Lambda]}r)\vec{A}_4 + I_1(\sqrt{[\Lambda]}r)\sin(\theta)\vec{A}_5 + I_1(\sqrt{[\Lambda]}r)\cos(\theta)\vec{A}_6 \\ & + K_1(\sqrt{[\Lambda]}r)\sin(\theta)\vec{A}_7 + K_1(\sqrt{[\Lambda]}r)\cos(\theta)\vec{A}_8 + zI_0(\sqrt{[\Lambda]}r)\vec{A}_9 + zK_0(\sqrt{[\Lambda]}r)\vec{A}_{10} \\ & + \sinh(\sqrt{[\Lambda]}z)\ln(r)\vec{A}_{11} + \cosh(\sqrt{[\Lambda]}z)\ln(r)\vec{A}_{12}, \end{aligned} \quad (3)$$

where \vec{A}_i , $i = 0, 1, \dots, 12$, are expansion coefficient vectors. \vec{A}_0 is a “slack” coefficient vector that goes to zero as the solution converges.

Note that each term in Eq. (3) is an analytic solution of Eq. (2). The thirteen coefficients in Eq. (3) are made to correspond to the thirteen nodal unknowns for a node : i) one node average flux, and ii) twelve half-interface average fluxes (two half-interface average fluxes for each of the six surfaces). Note that each term in Eq. (3) requires matrix functional evaluations (see Section 2.3).

2.2 Innermost Nodes

In an innermost node, the inner radial surface degenerates (disappears) into the z-axis and thus less nodal unknowns may be necessary. In addition, usually the innermost nodes are smaller in size. Moreover, some of the terms in Eq. (3) render the solution unbounded at $r=0$. Therefore, the terms that involve $G_0(\sqrt{[\Lambda]}r)$, $G_1(\sqrt{[\Lambda]}r)$, and $\ln(r)$ are excluded. The remaining seven coefficients are then made to correspond to : i) one node average flux, ii) two half-interface average fluxes on the outer radial surface, and iii) four surface average fluxes on the other surfaces.

2.3 Multi-group Extension

The eigenvalues of matrix $[\Lambda]$ are always real in two-group problems. But in multigroup problems, the eigenvalues can be complex. Instead of the transformation matrix approach in Ref. 6, the method for multigroup problems in this paper is based on the use of the spectral decomposition property in the matrix function theory[7]. The matrix function theory applies to the matrix functional evaluations of $f([\Lambda])$, where f is an analytic function and $[\Lambda]$ is a $G \times G$ matrix. According to the spectral decomposition property of the matrix function theory, we have

$$f([\Lambda]) = \sum_{i=0}^{G-1} b_i [\Lambda]^i, \quad (4)$$

where the decomposition coefficients b_i can be obtained from the following polynomial interpolation :

$$p(\lambda_k) = f(\lambda_k), \quad k = 0, 1, \dots, G-1, \tag{5}$$

where λ_k 's are the eigenvalues of $[\Lambda]$ (with complex conjugates allowed) and

$$p(\lambda) = \sum_{i=0}^{G-1} b_i \lambda^i. \tag{6}$$

Therefore, the matrix functions can be easily evaluated if the eigenvalues of the matrix $[\Lambda]$ are known.

2.4 Treatment of Void Regions

2.4.1 Partial Current Translation (PCT) Method

The typical pebble bed reactors (PBRs) have void regions in the top and side regions of the core. The finite difference method (FDM) used by the VENTURE code treats the void regions like the nodes whose diffusion coefficients are arbitrarily large and other cross sections are zero. However, if the diffusion coefficient is large, the FDM numerical scheme becomes erratic or very slow.

To treat the void regions, we introduce a partial current translation (PCT) method, which does not use diffusion coefficients. In Fig. 2, the idea of the PCT method is depicted; the outgoing current of region I is set to incoming current of region II :

$$A^I j_i^+ = A^{II} j_{ii}^-,$$

where A^I and A^{II} are surface areas of region I and II, respectively. Similarly,

$$A^I j_i^- = A^{II} j_{ii}^+.$$

Then, from the relations of diffusion theory,

$$\phi_i = 2(j_i^+ + j_i^-),$$

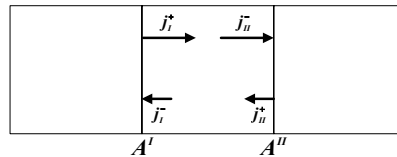
$$\phi_{ii} = 2(j_{ii}^+ + j_{ii}^-),$$

we have

$$A^I \phi_i = A^{II} \phi_{ii}.$$

Thus, now we can “jump” from region I to region II in computation as if there is no void region.

Figure 2: Partial current translation method



2.4.2 AFEN-based Method

The AFEN formulation for a void node starts from the following multi-group “diffusion” equations :

$$-[D]\nabla^2 \vec{\phi}(r, \theta, z) = 0. \tag{7}$$

The type of equations (7), i.e., Laplace equation, appears quite extensively in electromagnetic theory in physics[8]. Following the AFEN methodology, a general solution to Eq.(7) can be represented in terms of analytic basis functions that can be obtained using the method of separation

of variables :

$$\begin{aligned}
 \bar{\phi}(r, \theta, z) = & \bar{A}_0 + r\text{Sin}(\theta)\bar{A}_1 + r\text{Cos}(\theta)\bar{A}_2 + \frac{1}{r}\text{Sin}(\theta)\bar{A}_3 + \frac{1}{r}\text{Cos}(\theta)\bar{A}_4 \\
 & + \text{Sin}\left(\frac{z}{100}\right)I_0\left(\frac{r}{100}\right)\bar{A}_5 + \text{Cos}\left(\frac{z}{100}\right)I_0\left(\frac{r}{100}\right)\bar{A}_6 \\
 & + \text{Sin}\left(\frac{z}{100}\right)K_0\left(\frac{r}{100}\right)\bar{A}_7 + \text{Cos}\left(\frac{z}{100}\right)K_0\left(\frac{r}{100}\right)\bar{A}_8 \\
 & + z\bar{A}_9 + \text{Log}(r)\bar{A}_{10} + z\text{Log}(r)\bar{A}_{11}.
 \end{aligned} \tag{8}$$

Note that each term in Eq. (8) is an analytic solution of Eq. (7). We have 12 coefficients in Eq. (8), one coefficient less than in Eq.(3), with the same nodal unknowns but excepting the node average flux. This method still requires diffusion coefficients, but all other cross sections are zero. Suitable diffusion coefficients may be given for a void node from “equivalent” diffusion model.

3. TOPS Code

The AFEN method and the two void treatment methods described in Section 2 have been implemented in a code named TOPS [3]. After the coefficients in Eq. (3) are expressed in terms of the nodal unknowns, we build as many solvable nodal coupling equations as the number of these nodal unknowns to be determined. The nodal coupling equations in AFEN typically consist of the nodal balance equation and the two half-interface current continuity equations. For the boundary conditions, two options are available in the code : i) $\phi = 0$ and ii) $j^- = 0$.

4. Results and Discussion

The TOPS code was used to solve the OECD/PBMR-400 benchmark problem, shown in Fig. 4. It is a two-group problem with void regions above the annular core (top void) and between outer reflector (side void) and core barrel and $j^- = 0$ boundary condition (specified as BLACK boundary condition). Detailed configurations and cross sections are shown in Ref. [2]. Although Steady-State Exercise 1 is an (r-z) problem since the properties are constant in θ -direction, it is solved by the (r, θ ,z) TOPS code. The number of nodes used is 20x4x29 in (r- θ -z) directions, respectively. This is the coarsest node size configuration that is allowed as specified in the material regions.

To describe void regions, the OECD/NEA benchmark problem provided directional dependent diffusion coefficients: $D_{top-void}^r = 4.2789cm$, $D_{top-void}^z = 22.8055cm$, and $D_{side-void}^r = 0.268625cm$, $D_{side-void}^z = 8.280125cm$. The directional dependent diffusion coefficients purport to represent the neutron streaming effects in the diffusion calculation. In this paper, we used two ways of void treatment: i) use of PCT, ii) use of AFEN formulation. Table 1 shows the results on k_{eff} by TOPS with PCT void treatment and by VENTURE with a large diffusion coefficient (arbitrarily 10000cm) in void regions, where the diffusion coefficient should be infinite, to obtain more close reference. Table 2 shows a summary of the TOPS results with PCT void treatment.

Figure 4: OECD/PBMR-400 benchmark problem

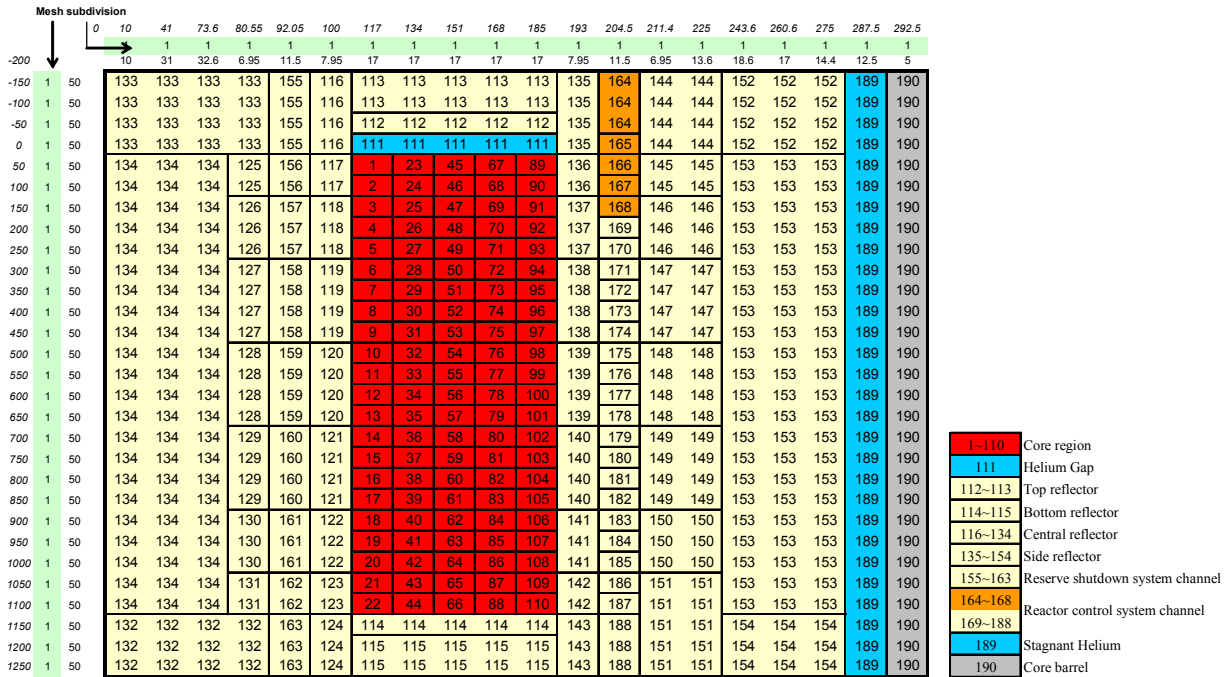


Table 1: Results of the OECD/PBMR-400 benchmark problem

	k_{eff}	diff. (pcm)
VENTURE ^a	0.99543	reference
TOPS ^b	0.99642	99

(a) r-z (580x2900) calculation with $D_{void}=10000\text{cm}$

(b) r- θ -z (20x4x29) calculation with PCT void method

Table 2: Summary of the TOPS Results (PCT void method)

	TOPS (PCT void method)
k-eff	0.99642
Maximum Power density (W/cm ³)	10.858559
Maximum fast flux (n/cm ² /s)	2.12E+14
Maximum thermal flux (n/cm ² /s)	3.33E+14
Leakage from core (% per one lost neutron)	1.52E+01
Leakage from calculational domain (% per one lost neutron)	4.19E-01

To verify the void treatment with AFEN formulation described in Section 2.4.2, fine mesh VENTURE reference calculation was performed. Because the VENTURE code does not support directional dependent diffusion coefficient option, we performed both TOPS and VENTURE calculations using r and z directional diffusion coefficients in the side and top void regions, respectively. Table 3 shows the results of the TOPS and VENTURE codes. They are in excellent agreement.

Table 3: Summary of the TOPS and VENTURE Results^a

	VENTURE ^b (reference)	TOPS ^c (AFEN void method)
k-eff	1.00461	1.00466 (+5pcm)
Maximum Power density (W/cm ³)	10.518072	10.526584
Maximum fast flux (n/cm ² /s)	2.07E+14	2.06E+14
Maximum thermal flux (n/cm ² /s)	3.23E+14	3.22E+14
Leakage from core (% per one lost neutron)	1.45E+01	1.45E+01
Leakage from calculational domain (% per one lost neutron)	1.68E-01	1.71E-01

(a) $D_{top_void} = 22.8055$ cm, $D_{side_void} = 0.268625$ cm

(b) r-z (580x2900) calculation

(c) r-θ-z (20x4x29) calculation

A summary of the TOPS results with directional dependent diffusion coefficients given in the benchmark specification is shown in Table 4 and the results in the table are our solution of the OECD/NEA PBMR-400 benchmark problem.

Table 4: TOPS solution of the OECD/NEA PBMR-400 benchmark problem^a

	TOPS (AFEN void method)
k-eff	1.00426
Maximum Power density (W/cm ³)	10.5433074
Maximum fast flux (n/cm ² /s)	2.07E+14
Maximum thermal flux (n/cm ² /s)	3.23E+14
Leakage from core (% per one lost neutron)	1.45E+01
Leakage from calculational domain (% per one lost neutron)	4.66E-01

(a) $D_{top-void}^r = 4.2789$ cm, $D_{top-void}^z = 22.8055$ cm, $D_{side-void}^r = 0.268625$ cm, $D_{side-void}^z = 8.280125$ cm.

5. Conclusions

Following a brief description of the AFEN method in cylindrical (r,θ,z) geometry, the paper presented preliminary results of the OECD/NEA PBMR-400 benchmark problem obtained by the TOPS code.

The multigroup extension and two void treatment methods using partial current translation (PCT) and AFEN formulation were described in the Section 2. When diffusion coefficients for void regions, actually infinite, are not provided, PCT void method could be used. Although the PCT method to treat void regions is simple to use and does not require the knowledge of diffusion coefficients, it does not account for “cross-fly” neutrons, thus causing some accuracy loss. When suitable diffusion coefficients of void regions are given, AFEN formulation described in Section 2.4.2 can be used. By comparing the results with the VENTURE code (Table 3), the TOPS results of AFEN formulation for void with diffusion coefficients are in excellent agreement with those of the VENTURE. From these results, it is judged that the TOPS code with the AFEN void method

seems to be a very accurate nodal code in cylindrical geometry, if the diffusion coefficients are appropriately provided for void regions.

After several verification results of the TOPS code, the OECD/NEA benchmark calculation was performed by TOPS using the AFEN void treatment with given directional dependent diffusion coefficients and the solution of the benchmark problem was presented. It is noted that the discrepancy in the k_{eff} results between the PCT and AFEN void methods is substantial.

Appendix (A modified PBMR benchmark problem)

As shown in Section 4, we have different results depending on the ways of treatment of the void regions and their differences are substantial ($\Delta k_{eff} = 784$ pcm). Thus, it would be better to have a benchmark problem which does not contain void regions to verify computational methods in cylindrical geometry, and to separate out the effect of the void regions. For this reason, we slightly modified the OECD PBMR400 benchmark problem. From the configurations in Fig. 4, the Helium gap (111) regions in upper part of the core were replaced by the neighbor graphite reflector (112) material, and the stagnant Helium (189) regions in the outside of the side reflector were replaced by the neighbor side reflector (152-154) material. Table 5 shows the results of the modified benchmark problem.

Table 5: Results of the modified OECD/PBMR-400 benchmark problem

Code used	Mesh division	k_{eff}	diff. (pcm)
VENTURE ^a	580x2900	1.00051	reference
	290x2900	1.00046	-5
	143x2900	1.00035	-16
	55x2900	0.99905	-146
	580x1450	1.00050	-1
	580x725	1.00050	-1
	580x290	1.00051	0
	580x145	1.00053	2
	580x58	1.00068	18
	20x29	0.99117	-933
TOPS ^b	20x4x116	1.00053	2
	20x4x58	1.00053	2
	20x4x29	1.00055	4

- (a) r-z mesh division
- (b) r-θ-z mesh division

We note from the results that the TOPS code gives very accurate solution even with the coarsest mesh division and the results show very small differences as refining the mesh division. For the results of the VENTURE code, Table 5 shows that the multiplication factor is rather insensitive in z-direction refinement so that we obtained multiplication factor of 2 pcm difference from the

reference even with 10cm size of z-direction mesh size, while about 2cm of r-direction mesh size was required for multiplication factor of 16pcm difference. This may be because the configuration of the benchmark problem is much longer in dimensions and more homogeneous in material regions axially than radially. It is also observed that the convergence directions are opposite in axial and radial mesh refinements.

We note from Tables 2, 4, and 5 that the effect of the presence of the void regions on k_{eff} is $\Delta k_{eff} = -413$ pcm and $\Delta k_{eff} = 371$ pcm by PCT and AFEN void treatments, respectively. The overprediction by the AFEN void treatment renders its validity of the result questionable, implying that appropriateness of the diffusion coefficients provided for the void regions is in doubt. In summary, this indicates that the effect of void regions is significant and that the method how to treat the voids in computation is important.

Acknowledgments

This work was supported in part by the Ministry of Science and Technology (MOST) of Korea through the Nuclear Hydrogen Development and Demonstration (NHDD) Project coordinated by Korea Atomic Energy Research Institute.

References

- 1) A. C. Kadak, D. A. Petti, *et al.*, "Modular Pebble Bed Reactor Project University Research Consortium Annual Report," INEEL/EXT-2000-01034, Idaho National Engineering & Environmental Laboratory (2000).
- 2) F. Reitsma, *et al.*, "PBMR Coupled Neutronics/Thermal Hydraulics Transient Benchmark The PBMR-400 Core Design – Benchmark Definition," NEA/NSC/DOC(2005)xxx Draft-V03, Nuclear Energy Agency, Organization for Economic/Cooperation and Development, September 1 (2005).
- 3) N. Z. Cho, *et al.*, "The Analytic Function Expansion Nodal (AFEN) Method in Cylindrical (r,θ,z) Geometry for Pebble Bed Reactors," *Trans. Am. Nucl. Soc.*, **93**, 624 (2005).
- 4) N. Z. Cho, *et al.*, "The AFEN Method in Cylindrical (r,θ,z) Geometry for Pebble Bed Reactors - Extension to Multigroup Form and Treatment of Voids -," *Trans. Am. Nucl. Soc.*, **94**, 553 (2006).
- 5) A. M. Ougouag and W. K. Terry, "Analytic Solution of the Neutron Diffusion Equation in Three-Dimensional Cylindrical Geometry for Application in a Nodal Method," *Proceedings of the Nuclear Mathematical and Computational Sciences: A Century in Review - A Century Anew (M&C 2003)*, Gatlinburg, TN, April 6-10 (2003).
- 6) N.Z. Cho, Y.H. Kim, and K.W. Park, "Extension of Analytic Function Expansion Nodal Method to Multigroup Problems in Hexagonal-Z Geometry," *Nucl. Sci. Eng.*, **126**, 35 (1997).
- 7) N. Dunford and J.T. Schwartz, "Linear Operators Part I: General Theory," Interscience Publishers, New York (1971).
- 8) J.D. Jackson, "Classical Electrodynamics," 2nd Edition, John Wiley & Sons, New York (1975).